



Journal of Applied and Computational Mechanics



Research Paper

Third-grade Fluid Flow of Stretching Cylinder with Heat Source/Sink

Aamir Ali¹ , Sana Mumraiz¹ , Sara Nawaz¹, Muhammad Awais¹, Saleem Asghar² 

¹ Department of Mathematics, COMSATS University Islamabad, Attock Campus, Kamra Road, Attock, 43600, Pakistan

² Department of Mathematics, COMSATS University Islamabad, Park Road, Chak Shehzad, Islamabad, 44000, Pakistan

Received October 02 2019; Revised January 06 2020; Accepted for publication February 04 2020.

Corresponding author: A. Ali (aamir_ali@cuiatk.edu.pk)

© 2020 Published by ShahidChamran University of Ahvaz

Abstract. In this research, the impact of heat transfer on mixed convection steady third-grade fluid flow over an impermeable stretching cylinder with heat source is scrutinized. The investigation of mixed convection with non-Newtonian fluid is significant in geophysical and engineering fields. Appropriate transformations are alleged to obtain ordinary differential equations, which are later computed by using an analytical approach called the homotopy analysis methodology (HAM), and the interval of convergence is computed. Local Nusselt number and coefficient of skin friction values are computed numerically for novel parameters.

Keywords: Incompressible fluid; Stretching cylinder; Third-grade fluid; Heat source/sink; Mixed convection.

1. Introduction

In recent years, non-Newtonian fluids have become significant in many industrial manufacturing techniques, particularly with the improvement of the polymer industry, petroleum industry, food, microfluid, fiber, and paper industries. Because of diverse physical nature, no general model available, which adequately describes the rheology of non-Newtonian fluids. The governing equations obtained are highly nonlinear. For these reasons, under realistic conditions, both the mathematical analysis and the numerical simulation of non-Newtonian fluids are very challenging. Three types of non-Newtonian fluids, namely the integral type, the rate type, and differential type fluids, also known as Rivlin-Ericksen tensor, is vital in fluid literature [1]. Differential-type fluids can be classified according to the order of the time derivatives of the velocity gradient that appear in the stress tensor. In particular, second-grade fluids reproduce the normal stress effects, but they do not influence shear thickening and shear thinning properties. To reproduce these phenomena, a velocity gradient of higher-order is required. Third-grade fluids are a subgroup of the family of fluids of intricacy three, which follow a particular constitutive law. The fluid model of third-grade contained all properties of viscoelastic fluids. This model anticipated the shear-thinning/thickening features along with normal stresses. The stability and thermodynamics of these fluids were examined by Fosdick and Rajagopal [2]. The capability of a third-grade phenomenon to explain the shear thickening/thinning characteristics for various flow configurations has motivated the investigators to probe this model under different physical situations. Hayat et al. [3] scrutinize the analytical study of axisymmetric boundary layer motion of third-grade fluid over stretching cylinder with magnetic effects. Rashidi et al. [4] have done significant analysis on entropy generation of convective third grade fluid motion over stretching sheet under the magnetic effects. Samuel et al. [5] analyzed the irreversibility theory in the reactive third grade fluid flow. Hayat et al. [6] examined the axisymmetric squeezing third grade fluid flow between two disks. Reddy et al. [7] explored the flow visualization of third grade fluid over heated cylinder by using theory of Bejan's heat function. They concluded that wall shear stress and coefficient of heat transport decays at the heated walls as third grade fluid parameter grows. Several recent studies regarding third grade fluid can be cited in [8-14].

Mixed convection is the heat transport process resulted by combined effects of forced convection and free convection. The significance of the stretched surface, along with mixed convection flow, has ample implementations in industry and engineering such as solar collectors, atomic reactors, electronic equipment, and heat exchanger. In light of all these applications, several investigations have been undertaken to examine the outcomes of mixed convection (See Refs [15-22]).

A heat generation/absorption is a system with a large heat capacity that its temperature remains constant when it is in contact with other systems. Heat source/sink crucially controls heat transfer. Freezers and air conditioning (AC) are common examples of heat source/sink, and these heat pumps are used in many heating, ventilation, and air conditioning (HVAC) devices. They are useful in electronics, e.g., in lasers, semiconductors, transistors, and optoelectronic devices. Hayat et al. [23] discussed the non-uniform heat generation/absorption and radiation effects over stretched cylinder immersed in a thermally stratified media. Srinivas et al. [24] obtained analytical results to study the impacts of chemical reaction and heat source/sink on magnetohydrodynamic (MHD) nanofluid motion in a stretching and shrinking permeable pipe. Irfan et al. [25] explored the 3D unsteady Carreau nanofluid transport numerically with variable thermal conductivity and generation/absorption heat influences. Khan et al. [26] highlighted the mixed convection couple stress fluid generated by oscillatory stretched sheet in the existence of nanoparticles. An investigation of Oldroyd-B nanofluid flow in the presence of generative/absorptive heat over stretching sheet has been done by Giressha et al.



[27]. Shamshuddin et al. [28] accounted the variable heat flux to capture the properties of micropolar fluid transport induced by permeable sheet. Ali et. al [29] studied the effects of non-uniform heat flux over exponentially stretching surface. Recently, Ali et al. [30] investigated the heat flux phenomenon between two rectangular plane walls which are expanding or contracting.

The main aim of the present study is to investigate the impact of heat transfer on mixed convection steady third-grade fluid flow over an impermeable stretching cylinder in the presence of heat source/sink. The governing equations with appropriate boundary conditions are transformed into ordinary differential equations, whose solution is computed by using an analytical approach called the homotopy analysis methodology (HAM), and the interval of convergence is computed. Local Nusselt number and coefficient of skin friction values are computed numerically for novel parameters. The effects of different involved parameters on the flow field of velocity and temperature distribution are analyzed with the help of graphs.

2. Mathematical Modeling

The steady, laminar, incompressible flow dynamics of third-grade fluid along with mixed convection is encountered. Flow phenomena occur due to the stretching cylinder of radius R with velocity $u_c(x)$ linearly related to axial distance x . The cylindrical coordinates system is taken such that x – axis is parallel to the axial direction of cylinder whereas r – axis is taken normal to it. $T_c(x)$ and T_∞ are the temperature at the surface and free stream respectively. Heat transfer phenomenon is studied in the occurrence of thermal conductivity which depends on temperature. The geometry of the problem is shown in Fig. 1.

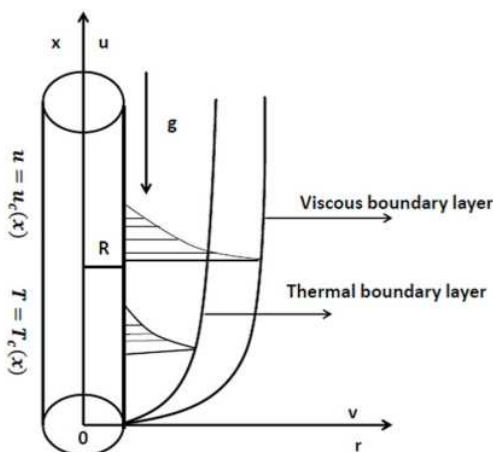


Fig. 1. Physical flow model

The velocity field in the cylindrical coordinate system is taken as:

$$\mathbf{V} = [v(r, x), 0, u(r, x)]. \tag{1}$$

The governing model under the Boussinesq and boundary layer approximation (i.e. $x = O(1), r = O(\delta), u = O(1), v = O(\delta)$) taken the form [7, 15, 16, 17]:

$$\frac{\partial(ru)}{\partial x} + \frac{\partial(rv)}{\partial r} = 0, \tag{2}$$

$$\begin{aligned} v \frac{\partial u}{\partial r} + u \frac{\partial u}{\partial x} &= v \left(\frac{\partial^2 u}{\partial r^2} + \frac{1}{r} \frac{\partial u}{\partial r} \right) + \frac{\alpha_1}{\rho} \left(\frac{u}{r} \frac{\partial^2 u}{\partial r \partial x} + \frac{v}{r} \frac{\partial^2 u}{\partial r^2} + \frac{3}{r} \frac{\partial u}{\partial r} \frac{\partial u}{\partial x} \right) \\ &+ \frac{1}{r} \frac{\partial v}{\partial r} \frac{\partial u}{\partial r} + 4 \frac{\partial u}{\partial r} \frac{\partial^2 u}{\partial r \partial x} + u \frac{\partial^3 u}{\partial r^2 \partial x} + 2 \frac{\partial v}{\partial r} \frac{\partial^2 u}{\partial r^2} + u \frac{\partial^3 u}{\partial r^3} + 3 \frac{\partial^2 u}{\partial r^2} \frac{\partial u}{\partial x} + \frac{\partial^2 v}{\partial r^2} \frac{\partial u}{\partial r} \\ &+ \frac{\alpha_2}{\rho} \left(\frac{2}{r} \frac{\partial v}{\partial r} \frac{\partial u}{\partial r} + \frac{2}{r} \frac{\partial u}{\partial r} \frac{\partial u}{\partial x} + 2 \frac{\partial^2 v}{\partial r^2} \frac{\partial u}{\partial x} + 2 \frac{\partial^2 u}{\partial r^2} \frac{\partial v}{\partial r} + 2 \frac{\partial^2 u}{\partial r^2} \frac{\partial u}{\partial x} + 4 \frac{\partial u}{\partial r} \frac{\partial^2 u}{\partial r \partial x} \right) \\ &+ \frac{\beta_3}{\rho} \left(\frac{2}{r} \left(\frac{\partial u}{\partial r} \right)^3 + 6 \left(\frac{\partial u}{\partial r} \right)^2 \frac{\partial^2 u}{\partial r^2} \right) - g \beta_T (T - T_\infty), \end{aligned} \tag{3}$$

$$v \frac{\partial T}{\partial r} + u \frac{\partial T}{\partial x} = \frac{1}{\rho c_p r} \frac{\partial}{\partial r} \left(K(T) r \frac{\partial T}{\partial r} \right) + \frac{Q(T - T_\infty)}{\rho c_p}. \tag{4}$$

The associated boundary conditions are [15]:

$$u(x, R) = u_c(x) = \frac{u_0 x}{l}, v(x, R) = 0, T(x, R) = T_c(x) = T_\infty + \left(\frac{x}{l} \right)^n \Delta T, \tag{5}$$

$$u(x, r) \rightarrow 0, T(x, r) \rightarrow T_\infty, \quad \text{as } r \rightarrow \infty.$$



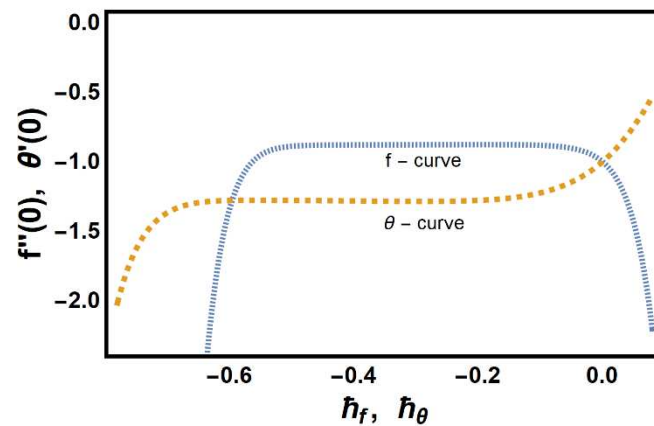


Fig. 2. h - curves for f and θ

In the above expressions, components of velocity along (x, r) axes are u and v respectively, ν is named as kinematic viscosity, ρ is called fluid density, α_1, α_2 and β_3 are the second and third-grade fluid parameters, β_1 the volumetric thermal expansion, T is the fluid temperature, n is temperature exponent, c_p named as specific heat, $K(T) = K_\infty(1 + \varepsilon\theta)$ stands for variable thermal conductivity, where K_∞ is fluid thermal conductivity at free stream, ε denotes variable thermal conductivity parameter, θ is the dimensionless temperature, Q is the generation/absorption heat parameter. Moreover, $u_c(x), u_0$ expresses the stretching and reference velocity and $l, \Delta T$ is characteristics length and characteristic temperature. Following similarity transformation are introduced [13]:

$$\eta = \sqrt{\frac{u_0}{\nu l}} \left(\frac{r^2 - R^2}{2R} \right), u = \frac{u_0 x}{l} f'(\eta), v = -\frac{R}{r} \sqrt{\frac{u_0 \nu}{l}} f(\eta), \theta(\eta) = \frac{T - T_\infty}{T_c - T_\infty}. \quad (6)$$

Employing Eq. (6) in Eqs. (2)-(5), we obtained:

$$(1 + 2\gamma\eta)f'''' + 2\gamma f'' + ff'' - f'^2 + \alpha_1 [2(1 + 2\gamma\eta)ff'''' - ff^{(iv)} + 3f''^2 + \eta(6ff'' - 2ff''')] + \alpha_2 [2(1 + 2\gamma\eta)f''^2 + \gamma(2ff'' + 2ff''')] + \beta_3 \text{Re} [6(1 + 2\gamma\eta)^2 f''^2 f'''' + 8\gamma(1 + 2\gamma\eta)f''^3] - \lambda\theta = 0, \quad (7)$$

$$(1 + 2\gamma\eta)(1 + \varepsilon\theta)\theta'' + 2\gamma(1 + \varepsilon\theta)\theta' + \varepsilon(1 + 2\gamma\eta)\theta'^2 + \text{Pr}(f\theta' - nf'\theta) + h_s\theta = 0, \quad (8)$$

$$\begin{aligned} f(0) = 0, f'(0) = 1, \theta(0) = 1, \\ f'(\eta) \rightarrow 0, \theta(\eta) \rightarrow 0 \text{ as } \eta \rightarrow \infty. \end{aligned} \quad (9)$$

In above equations the non-dimensional parameters are γ the curvature parameter, α_1, α_2 and β_3 are the second and third-grade fluid parameters, λ the mixed convection parameter, Re the Reynolds number, Pr the Prandtl number and h_s the heat source/sink parameter and mathematically stated as:

$$\begin{aligned} \gamma = \sqrt{\frac{\nu l}{u_0 R^2}}, \alpha_1 = \frac{\alpha_1 u_0}{\mu l}, \alpha_2 = \frac{\alpha_2 u_0}{\mu l}, \beta_3 = \frac{\beta_3 u_0^2}{\mu l}, \\ \lambda = \frac{g\beta_1 l^2 (T_c - T_\infty)}{u_0^2 x}, \text{Re} = \frac{u x}{\nu}, \text{Pr} = \frac{\mu c_p}{K_\infty}, h_s = \frac{Q l}{u_0 \rho c_p}. \end{aligned} \quad (10)$$

The skin friction coefficient C_f and Nusselt number Nu_x are given by the expressions:

$$C_f = \frac{2\tau_c}{\rho u_c^2}, Nu_x = \frac{x q_c}{K_\infty (T_c - T_\infty)}, \quad (11)$$

In Eq. (11), τ_c and q_c represents the shear stress at the wall and heat flux which are formulated as:

$$\tau_c = \left[\mu \frac{\partial u}{\partial r} + \alpha_1 \left[u \frac{\partial^2 u}{\partial r \partial x} + \nu \frac{\partial^2 u}{\partial r^2} + 3 \frac{\partial u}{\partial r} \frac{\partial u}{\partial x} + \frac{\partial v}{\partial r} \frac{\partial u}{\partial r} \right] + \alpha_2 \left[2 \frac{\partial v}{\partial r} \frac{\partial u}{\partial r} + \frac{\partial u}{\partial r} \frac{\partial u}{\partial x} \right] + 2\beta_3 \left(\frac{\partial u}{\partial r} \right)^3 \right]_{r=R}, q_c = -K_\infty \left(\frac{\partial T}{\partial r} \right)_{r=R}. \quad (12)$$

Using Eq. (12) into Eq. (11), we acquire the following terms for coefficient of skin friction and Nusselt number,

$$\text{Re}_x^2 C_f = f''(0) + 3\alpha_1 f''(0) + 2\beta_3 f''^3(0), \text{Re}_x^{-1/2} Nu_x = -\theta'(0). \quad (13)$$

In which $\text{Re}_x = ux / \nu$ is the local Reynolds number.



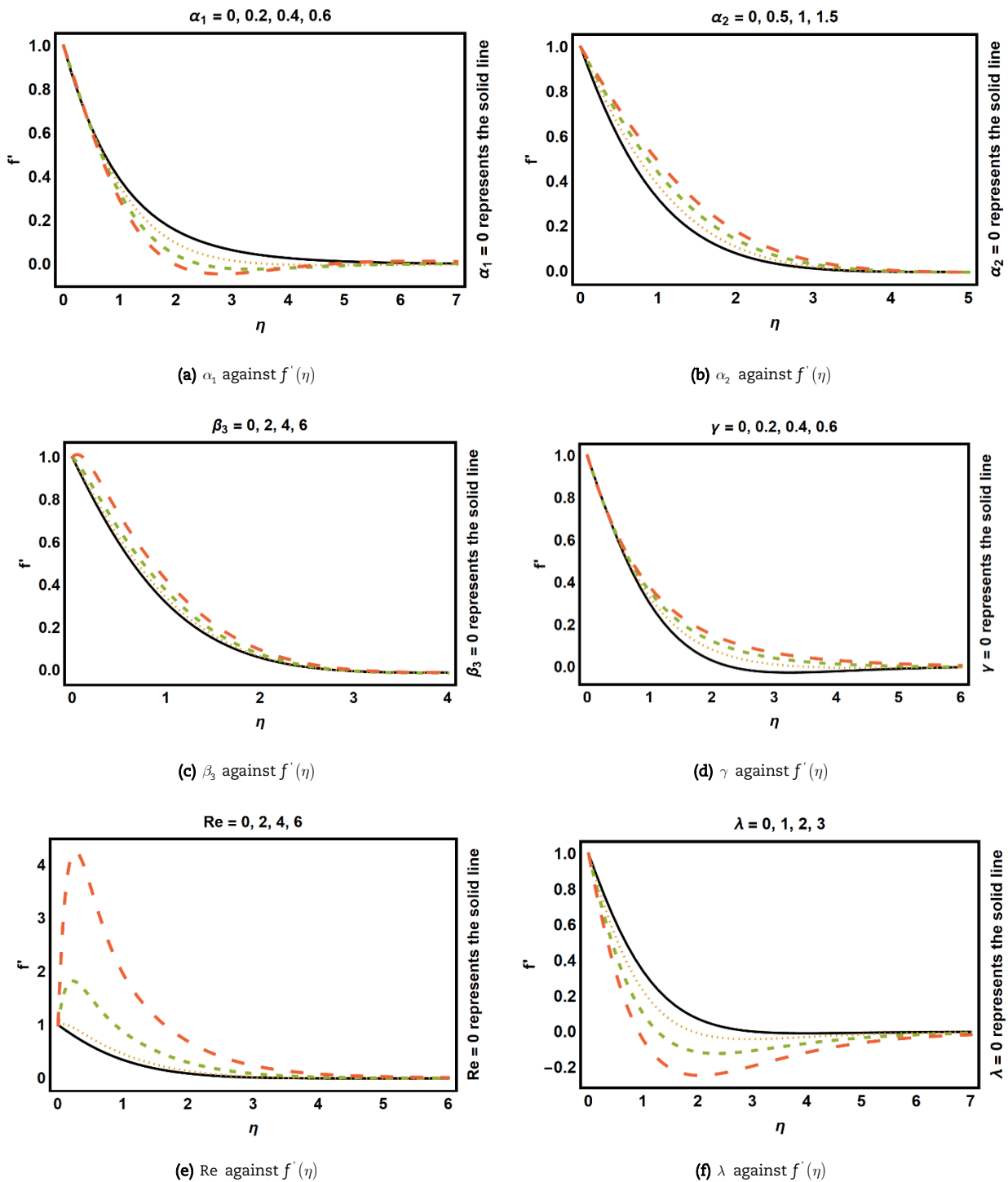


Fig. 3. Velocity profile for different parameters

3. Result and Discussion

Equations (7) and (8) with the boundary conditions (9) have been simplified analytically by utilization homotopy analysis methodology (HAM). For ranges of auxiliary parameters h_f and h_θ , we have sketched h – curves up to 13th approximation order in Fig. 2. We can see that the values of h_f and h_θ lies between $-0.6 \leq h_f \leq 0.05$ and $-0.75 \leq h_\theta \leq -0.1$. Explanation of the series solutions under the effect of different novel parameters on the flow and temperature distributions are analyzed in this portion. To examine the influence of sundry parameters on the velocity profile $f'(\eta)$, Fig. 3 (a) -3 (f) are sketched. Fig. 3 (a) manifests the impact of second-grade fluid parameter (α_1) against the velocity profile. The velocity decreases near the wall, and it exhibits mingling behavior away from the wall when $\eta \geq 5$. Also, the thickness of the momentum boundary layer is decreased. Fig. 3 (b) shows the variation of $f'(\eta)$ against the second-grade fluid parameter (α_2). It is observed that velocity is an increasing function of α_2 . The role of third-grade fluid (β_3) on $f'(\eta)$ is highlighted in Fig. 3 (c). It explores that for large value of β_3 the velocity increases close to the wall, and it disappears far off from it. Also, the momentum boundary layer thickness increases. Indeed, β_3 is related inversely to the viscosity. Increment in β_3 , causes fluid viscosity to diminish, and hence velocity profile increased.



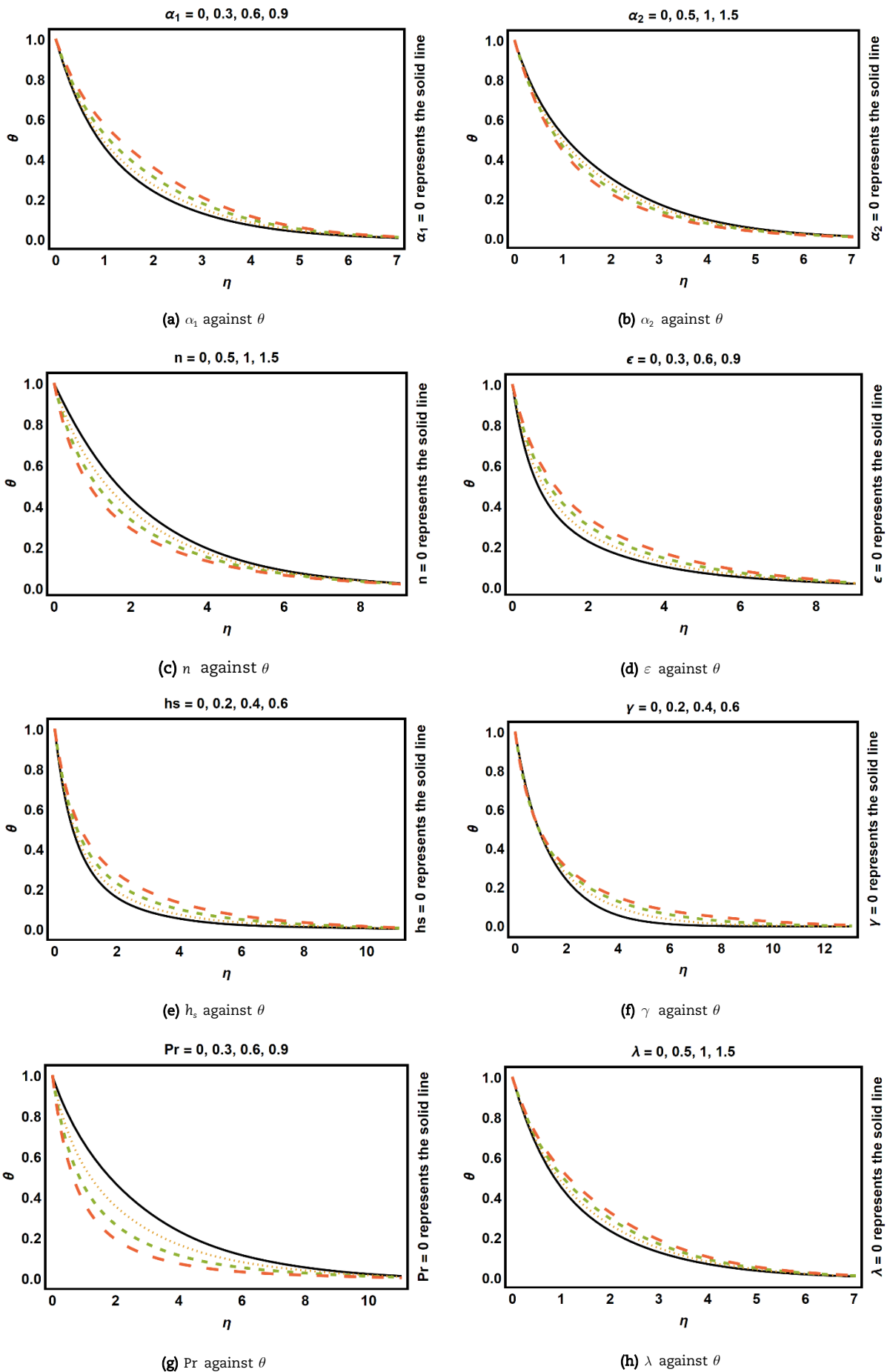


Fig. 4. Temperature profile for different parameters



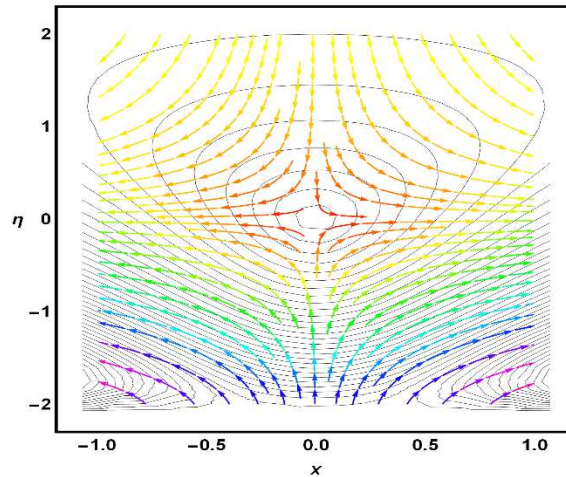


Fig. 5. Flow streamlines for two dimensionless flow.

Table 1. Numerical values of Nusselt numbers and skin friction for various parameters.

α_1	α_2	β_3	ε	Re	λ	Pr	γ	n	$-\text{Re}_x^{\frac{1}{2}} C_f$	$-\theta'(0)$
0.0	0.2	0.05	0.2	0.5	0.2	0.8	0.2	2	0.84060	1.3344
0.1									0.99830	1.3511
0.2									1.1419	1.3648
0.3									1.2604	1.3761
0.1	0.0								1.0863	1.3360
	0.1								1.0401	1.3438
	0.2								0.99834	1.3511
	0.3								0.96037	1.3581
	0.2	0.0							0.98928	1.3496
		0.1							1.0066	1.3527
		0.2							1.1880	1.3572
		0.3							1.9023	1.3525
		0.05	0.0						1.6775	1.4620
			0.2						2.6276	1.4830
			0.4						2.5691	1.4404
			0.2	0.4					0.86642	1.3508
				0.5					0.86441	1.3511
				0.6					0.86246	1.3514
				0.7					0.86018	1.3518
				0.5	0.0				1.8657	1.3401
					0.2				1.9023	1.3574
					0.4				2.6567	1.3767
					0.4	0.5			1.0459	1.0039
						0.8			0.98471	1.1976
						1.0			0.99834	1.3511
						1.0	0.1		0.95131	1.3128
							0.2		0.99830	1.3511
							0.3		1.0440	1.3887
							0.4		1.0882	1.4251
							0.4	0.0	1.0257	0.6264
								1.0	1.0665	1.0905
								2.0	1.0872	1.4231

Fig. 3 (d) represents the effect of curvature parameter (γ) against $f'(\eta)$. It is seen that increasing values of γ , decreases the velocity near the cylinder surface and strengthen the velocity and momentum boundary layer thickness far away from it. Physically, the main reason behind this is that, as the curvature parameter is inversely related to the curvature radius. Increment in γ diminish the cylinder radius, consequently, the contact region between liquid and cylinder alleviates, which increases the fluid motion and eventually enhances the velocity profile. The behavior of Reynolds number (Re) is portrayed in Fig. 3 (e), which discloses that $f'(\eta)$ increase by enhancing Re. The Reynolds number is termed as the fraction of inertial forces to viscous forces and for large values of Re the inertial forces became dominant as compared with viscous forces. Thus the velocity profile increases. Effect of mixed convection parameter (λ) against velocity is sketched in Fig. 3 (f). Decreasing trend is seen for both velocity and thickness of the velocity boundary layer for large value of λ .

Figures 4 (a) – 4 (h) presented the role of sundry parameters against temperature distribution. The influence of second-grade fluid parameter (α_1) against $\theta(\eta)$ is illustrated in Fig. 4 (a). We noted that temperature distribution enlarges close to the surface but more sensitive to increase away from it. Fig. 4 (b) represents the impact of second-grade parameter α_2 versus temperature $\theta(\eta)$. It describes that temperature decreases in the boundary layer, consequently thinning the thickness of the boundary layer. The variation of $\theta(\eta)$ versus temperature exponent (n) is illustrated in Fig. 4 (c). The result indicates that temperature, together with their corresponding boundary layer thickness decreases. Physically, this behavior presented that augmentation in n increases the difference between ambient temperature and wall, which boosted the rate of heat transfer, thus temperature decreases. Effect of variable thermal



conductivity parameter (ε) is plotted in Fig. 4 (d). Clearly, enhancement in thickness of thermal boundary layer and temperature is observed. As thermal conductivity relies on temperature, amplitude of temperature grows by rising average thermal conductivity. Fig. 4 (e) presented the impact of heat absorptive/generative parameter (h_s) against the temperature field. The figure shows that temperature increases for higher values of h_s . As the presence of thermal source delivered more heat that's why temperature field enhanced. Influence of curvature parameter (γ) versus $\theta(\eta)$ is demonstrated in Fig. 4 (f), which testified that near the wall thickness of thermal boundary layer and temperature decreases and increases away from the cylinder surface. Increment in γ enhances the rate of heat transfer from cylinder to the surface thus temperature field drop near the surface and strengthen away from region. Fig. 4 (g) is designed to explore the influence of Pr on $\theta(\eta)$. It reveals that increment in Pr diminished the temperature and thickness of thermal boundary layer. As Pr is proportion of mass diffusion to thermal diffusion. Increment in Pr slow down the heat diffusion rate due to which thermal boundary layer became thinner and temperature descended. Fig. 4 (h) is drawn to examine the variation in temperature profile for mixed convection parameter (λ) and reveals increasing behavior.

Streamlines for the given non-Newtonian, two-dimensional flow of third-grade fluid are presented in Fig. 5 for fixed values of parameters as $\alpha_1 = \alpha_2 = \gamma = \text{Re} = 0.1$, $\beta_3 = 0.2$, $v = l = U = r = 0.1$.

Table 1 represents the numerical values of the skin friction coefficient and heat transfer rate for various novel parameters. Observation concluded that increment in values of α_1 , β_3 , λ , γ , ε and n , intensified the coefficient of skin friction whereas it depressed with rise of α_2 , Re and Pr. Moreover, an expansion in Nusselt number is noticed for rising values of α_1 , α_2 , β_3 , λ , ε , γ , n , Re and Pr.

4. Conclusion

In this paper, third-grade fluid motion of stretching cylinder with heat source was studied, and the effects of different parameters on temperature and velocity profiles were discussed. Following are the observations of the problem:

- An increase in velocity was observed as the third-grade parameter was increased.
- Reynolds number has increasing effects on the velocity profile.
- The mixed convection parameter tends to decrease the velocity profile, but it increases the temperature profile.
- An increase in the curvature of the cylinder leads to more velocity and temperature.
- Heat source is providing heat to the system; that is why it increases the thermal boundary layer.
- Thermal conductivity (ε), and second-grade parameter (α_1) enhances the temperature field.
- For higher values of α_2 velocity field enlarges, but the opposite trend is observed for temperature.
- Rising values of n and Pr decrease the temperature profile.

Author Contributions

A. Ali planned the scheme, initiated the problem; S. Mumraiz has done the mathematical modeling of the problem; S. Nawaz found the solution and examined the theory validation; M. Awais verified the obtained results; S. Asghar contributed to the physical reasoning of the results. The manuscript was written through the contribution of all authors. All authors discussed the results, reviewed, and approved the final version of the manuscript.

Conflict of Interest

The authors declared no potential conflicts of interest with respect to the research, authorship, and publication of this article.

Funding

The authors received no financial support for the research, authorship, and publication of this article.

References

- [1] Dunn, J.E., Rajagopal, K.R., Fluids of differential type: critical review and thermodynamic analysis, *International Journal of Engineering Science*, 33, 1995, 689-729.
- [2] Fosdick, R.L., Rajagopal, K.R., Thermodynamics and stability of fluids of third grade, *Proceeding of Royal Society A*, 369, 1980, 351-377.
- [3] Hayat, T., Shafiq, A., Alsaedi, A., MHD axisymmetric flow of third grade fluid by a stretching cylinder, *Alexandria Engineering Journal*, 54, 2015, 205-212.
- [4] Rashidi, M.M., Bagheri, S., Momoniat, E., Freidoonimehr, N., Entropy analysis of convective MHD flow of third grade non-Newtonian fluid over a stretching sheet, *Ain Shams Engineering Journal*, 8, 2017, 77-85.
- [5] Adesanya, S.O., Falade, J.A., Jangili, S., Beg, O.A., Irreversibility analysis for reactive third grade fluid flow and heat transfer with convective wall cooling, *Alexandria Engineering Journal*, 56, 2017, 153-160.
- [6] Hayat, T., Nazar, H., Imtiaz, M., Alsaedi, A., Ayub, M., Axisymmetric squeezing flow of third grade fluid in presence of convective conditions, *Chinese Journal of Physics*, 55, 2017, 738-754.
- [7] Reddy, G.J., Hiremath, A., Kumar, M., Computational modeling of unsteady third grade fluid flow over a vertical cylinder: A study of heat transfer visualization, *Results in Physics*, 8, 2018, 671-682.
- [8] Ali, A., Saba, S., Asghar, S., Khan Marwat, D.N., Transport phenomenon in a third grade fluid over an oscillating surface, *Journal of Applied Mechanics and Technical Physics*, 58, 2017, 990-996.
- [9] Ali, A., Asghar, S., Vincenzi, D., Mixed convection of a conducting third grade fluid past an oscillating porous plate, *Journal of Engineering Thermophysics*, 26, 2017, 60-68.
- [10] Hayat, T., Khan, M.I., Waqas, M., Alsaedi, A., Magnetohydrodynamic stagnation point flow of third grade liquid toward variable sheet thickness, *Neural Computing, and Applications*, 30, 2018, 2417-2423.
- [11] Shah, Z., Gul, T., Islam, S., Khan, M.A., Bonyah, E., Hussain, F., Mukhtar, S., Ullah, M., Three dimensional third grade nanofluid flow in a rotating system between parallel plates with Brownian motion and thermophoresis effects, *Results in Physics*, 10, 2018, 36-45.
- [12] Khan, Z., Shah, R.A., Altaf, M., Islam, S., Khan, A., Effect of thermal radiation and MHD on non-Newtonian third grade fluid in wire coating analysis with temperature dependent viscosity, *Alexandria Engineering Journal*, 57, 2018, 2101-2112.
- [13] Hayat, T., Ahmad, S., Khan, M.I., Alsaedi, A., Modeling and analyzing flow of third grade nanofluid due to rotating stretchable disk with chemical reaction and heat source, *Physics B*, 537, 2018, 116-126.



- [14] Khan, M.I., Khan, S.A., Hayat, T., Alsaedi, A., Entropy optimization in magnetohydrodynamic flow of third grade nanofluid with viscous dissipation and chemical reaction, *Iranian Journal of Science and Technology, Transactions A: Science*, 43, 2019, 2679-2689.
- [15] Mukhopadhyay, S., Ishak, A., Mixed convection flow along a stretching cylinder in a thermally stratified medium, *Journal of Applied Mathematics*, 2012, 2012, Article ID 491695.
- [16] Hayat, T., Anwar, M.S., Farooq, M., Alsaedi, A., Mixed convection flow of viscoelastic fluid by a stretching cylinder with heat transfer, *Plos One*, 10, 2015, e0118815.
- [17] Hayat, T., Hussain, Z., Alsaedi, A., Farooq, M., Magnetohydrodynamic flow by a stretching cylinder with Newtonian heating and homogeneous-heterogeneous reactions, *Plos One*, 11, 2016, e0156955.
- [18] Hayat, T., Ullah, I., Ahmed, B., Alsaedi, A., MHD mixed convection flow of third grade liquid subject to nonlinear thermal radiation and convective condition, *Results in Physics*, 7, 2017, 2804-2811.
- [19] Rehman, K.U., Malik, A.A., Malik, M.Y., Sandeep, N., Saba, N.U., Numerical study of double stratification in Casson fluid flow in the presence of mixed convection and chemical reaction, *Results in Physics*, 7, 2017, 2997-3006.
- [20] Patil, P.M., Latha, D.N., Roy, S., Momoniati, E., Non-similar solutions of mixed convection flow from an exponentially stretching surface, *Ain Shams Engineering Journal*, 8, 2017, 697-705.
- [21] Hayat, T., Kiyani, M.Z., Alsaedi, A., Khan, M.I., Ahmad, I., Mixed convection three-dimensional flow of Williamson nanofluid subject to chemical reaction, *International Journal of Heat and Mass Transfer*, 127, 2018, 422-429.
- [22] Golafshan, B., Rahimi, A.B., Effects of radiation on mixed convection stagnation-point flow of MHD third grade nanofluid over a vertical stretching sheet, *Journal of Thermal Analysis and Calorimetry*, 135, 2019, 533-549.
- [23] Hayat, T., Asad, S., Alsaedi, A., Non-uniform heat source/sink and thermal radiation effects on the stretched flow of cylinder in a thermally stratified medium, *Journal of Applied Fluid Mechanics*, 10, 2016, 915-924.
- [24] Srinivas. S., Vijayalakshmi, A., Reddy, A.S., Ramamohan, T.R., MHD flow of a nanofluid in an expanding or contracting porous pipe with chemical reaction and heat source/sink, *Propulsion and Power Research*, 5, 2016, 134-148.
- [25] Irfan, M., Khan, M., Khan, W.A., Numerical analysis of unsteady 3D flow of Carreau nanofluid with variable thermal conductivity and heat source/sink, *Results in Physics*, 7, 2017, 3315-3324.
- [26] Khan, S.U., Shehzad, S.A., Rauf, A., Ali, N., Mixed convection flow of couple stress nanofluid over oscillatory stretching sheet with heat absorption/generation effects, *Results in Physics*, 8, 2018, 1223-1231.
- [27] Gireesha, B.J., Kumar, K.G., Ramesh, G.K., Prasannakumara, B.C., Nonlinear convective heat and mass transfer of Oldroyd-B nanofluid over a stretching sheet in the presence of uniform heat source/sink, *Results in Physics*, 9, 2018, 1555-1563.
- [28] Shamsuddin, M.D., Thirupathi, T., Satya Narayana, P.V., Micropolar fluid flow induced due to a stretching sheet with heat source/sink and surface heat flux boundary condition effects, *Journal of Applied and Computational Mechanics*, 5, 2019, 816-826.
- [29] Ali, A., Sajjad, A., Asghar, S., Thermal-diffusion, and diffusion-thermo effects in a nanofluid flow with non-uniform heat flux and convective walls, *Journal of Nanofluids*, 8, 2019, 1367-1372.
- [30] Ali, A., Iqbal, F., Khan Marwat, D.N., Asghar, S., Awais, M., Soret, and Dufour effects between two rectangular plane walls with heat source/sink, *Heat Transfer – Asian Research*, 49, 2020, 614-625.

ORCID iD

Aamir Ali  <https://orcid.org/0000-0002-6876-693X>

Sana Mumraiz  <https://orcid.org/0000-0002-7100-1524>

Saleem Asghar  <https://orcid.org/0000-0001-8453-4699>



© 2020 by the authors. Licensee SCU, Ahvaz, Iran. This article is an open access article distributed under the terms and conditions of the Creative Commons Attribution-NonCommercial 4.0 International (CC BY-NC 4.0 license) (<http://creativecommons.org/licenses/by-nc/4.0/>).

How to cite this article: Ali A., Mumraiz S., Nawaz S., Awais M., Asghar S. Third-grade Fluid Flow of Stretching Cylinder with Heat Source/Sink, *J. Appl. Comput. Mech.*, 6(SI), 2020, 1125–1132. <https://doi.org/10.22055/JACM.2020.31275.1850>

